JOURNAL OF GEOPHYSICAL RESEARCH, VOL. 105, NO. E7, PAGES 17,655–17,667, JULY 25, 2000

Relative timing of crustal plateau magmatism and tectonism at Tellus Regio, Venus

Brian K. Banks[1] and Vicki L. Hansen

Department of Geological Sciences, Southern Methodist University, Dallas, Texas

Abstract. Crustal plateaus, subcontinent-sized regions of thickened crust that stand 1-4 km above surrounding low-lying plains, define a major physiographic province of Venus. Thus their mode of emplacement plays a fundamental part in the evolution of the entire planet. Local topographic lows up to several hundred kilometers across filled with radar-dark volcanic flows, termed intratessera floodlava basins (ITBs), are common within crustal plateaus. ITBs record abundant crustal plateau volcanism and have implications for crustal plateau emplacement and evolution. We ask the fundamental question: Did ITBs develop before, during, or after crustal plateau development? To address this question, we mapped in detail the geology a particular ITB in Tellus Regio to determine temporal relationships between ITB volcanic flows and local crustal plateau tectonism. Mechanical arguments and crosscutting relationships indicate that ITB volcanism occurred during crustal plateau formation. Extending the timing relationships resolved at this basin, we suggest that ITB magmatism played a major role in crustal plateau genesis. The geologic history discerned is consistent with the upwelling model for crustal plateau evolution in which early surface extension and volcanism would be expected in a hotspot environment. Conversely, early widespread extension and volcanism would not be expected if crustal plateaus formed above a mantle downwelling because (1) predicted horizontal and radial convergence would obstruct early surface extension and (2) lower than normal geothermal gradients would impede, rather than enhance, volcanism.

1. Introduction

Crustal plateaus on Venus are steep-sided, flat-topped, quasi-circular highland regions of thickened crust ~1000-3000 km across that rise up to 4 km above surrounding radar-dark, low-lying volcanic plains [*Phillips and Hansen*, 1994]. Workers currently recognize seven crustal plateaus: eastern Ovda, western Ovda, Thetis, Tellus, Fortuna, Alpha, and Phoebe [*Hansen et al.*, 1999]. Although workers agree that crustal plateaus are regions of thickened crust [*Smrekar and Phillips*, 1991; *Bindschadler et al.*, 1992a; *Grimm*, 1994; *Simons et al.*, 1997], they disagree on the thickening mechanism. Two popular models currently exist: a mantle downwelling (coldspot) model and a revised mantle upwelling (hotspot) model. In the downwelling model, subsolidus flow of lower crustal material initiated by the negative buoyancy of a mantle coldspot results in lateral crustal accretion [*Bindschadler and Parmentier*, 1990; *Bindschadler et al.*, 1992a]. The revised upwelling model calls for crustal thickening by magmatic underplating and accretion above a hot mantle plume [*Phillips and Hansen*, 1998; *Hansen and Willis*, 1998]. Because crustal plateaus define a major physiographic province of Venus, their mode of formation plays a fundamental part in the evolution of the entire planet.

Tessera terrain, the dominant tectonic fabric of crustal plateaus, displays two or more intersecting structural elements [*Barsukov et al.*, 1986; *Basilevsky et al.*, 1986], the morphology and spatial patterns of which record surface strain. Workers have documented consistent temporal relationships between sets of tectonic elements common to crustal plateaus, forming the foundation for the revised upwelling model [*Hansen and Willis*, 1996, 1998; *Ghent and Hansen*, 1999]. Many of the timing relations that support mantle upwelling stem from mechanical analysis of secondary (i.e., tectonic) structures. Although these relationships provide compelling evidence for the revised upwelling model [*Hansen et al.*, 1999, 2000], many questions remain unanswered, and the debate of crustal plateau evolution continues. Additional constraints are required to fill in details of plateau developmental history.

Radar-dark regions spanning tens of thousands of square kilometers are common on crustal plateaus [e.g., *Bindschadler and Head*, 1991; *Bindschadler et al.*, 1992a, 1992b; *Gilmore and Head*, 1993, 1994; *Head*, 1995; *Banks and Hansen*, 1998a, 1999]. Workers have assumed a volcanic origin for these features [e.g., *Bindschadler et al.*, 1992 a, 1992b; *Gilmore and Head*, 1993, 1994; *Phillips and* Hansen, 1994; *Head*, 1995]. We interpret them to be volcanic based on the following: (1) their characteristic radar-dark signatures, when considered with the fact that they occupy local paleotopographic basins, suggest emplacement of smooth material restricted to local topographic lows by gravity, and (2) the two gravity-constrained processes that could result in localized deposition of smooth material into topographic lows are sedimentation and volcanism; because erosion, necessary for sedimentation, is probably not significant on Venus even at geologic timescales [*Sharpton and Head*, 1985; *Bindschadler and Head*, 1988; *Kaula*, 1990] and volcanism is common on Venus [e.g., *Head et al.*, 1992], radar-dark basins are likely filled with low

[1]Now at Law Engineering and Environmental Services Inc., Raleigh, North Carolina.

Paper number 1999JE001205.
0148-0227/00/1999JE001205$09.00

viscosity lava that solidified with a smooth surface. The association of volcanic edifices with these areas is consistent with this interpretation. We refer to these local topographic basins together with the dark material they contain as intratessera flood lava basins (ITBs).

ITB deposits, previously recognized in Pioneer-Venus, Venera, and Magellan data, have been referred to as "plains" [*Bindschadler et al.*, 1992a], "intratessera plains" [*Bindschadler and Head*, 1991; *Bindschadler et al.*, 1992b; *Gilmore and Head*, 1994; *Ivanov and Head*, 1996; *Hansen et al.*, 1997], "inter-tessera plains" [*Gilmore and Head*, 1993], and "intratesseral plains" [*Phillips and Hansen*, 1994]. The term "plains," with reference to Venus, typically implies the vast expanse of lowland volcanic plains that cover much of Venus' surface [e.g., *Banerdt et al.*, 1997]. Because many workers consider ITBs to be plains units, it is important to emphasize that ITB volcanism need not have been genetically related to regional plains emplacement. We avoid this a priori assumption by shedding the term "plains" with reference to ITB deposits. We use the modifier "intra" instead of "inter" because these deposits occur within, rather than between, the tessera terrain of individual crustal plateaus. We adopt the term "basin" to indicate the existence of a local paleotopographic low within which flood lava emplacement occurred.

The widespread occurrence of ITBs on crustal plateaus indicates abundant magmatism, which may have implications for crustal plateau genesis depending on the relative timing of ITBs with respect to crustal plateau formation. The interaction between crustal plateau magmatism and tectonism provides temporal constraints for plateau evolution independent of previous temporal studies. In this paper we examine in detail the geology of a particular ITB within Tellus, a crustal plateau in Venus' northern hemisphere, in order to determine its geologic history, which in turn allows us to address the fundamental questions: Did ITB magmatism occur before, during, or after crustal plateau tectonism; and what are the implications for crustal plateau evolution?

2. Background

Tellus Regio and the adjacent tesscra inlier, Meni Tessera, together define a quasi-circular highland region ~1600 by 2600 km located in Venus' northern hemisphere (Figure 1). A radar-dark, lava-flooded regional topographic low separates Meni Tessera to the north from the majority of Tellus Regio to the south. Some workers do not include Meni Tessera as part of Tellus [e.g., *Bindschadler et al.*, 1992a]; however, the spatial position, shape, topography, and strain patterns of Meni Tessera are contiguous with Tellus tessera (Figure 1), consistent with the interpretation that they together comprise a single crustal platcau that we refer to as Tellus.

Tellus' altimetry sampled on a 0.5° x 0.5° grid and contoured at 1-km intervals displays relatively large topographic gradients compared to adjacent gently sloping plains (Figure 1b). Tellus' central plateau rises >1 km above mean planetary radius (MPR) and ~2 km above surrounding regional plains that generally slope away from the plateau margins. The margins of Tellus sit slightly higher, on average, than the central plateau. Tellus' eastern boundary rises >2 km above MPR. Elevation profiles show the characteristic platcau morphology of Tellus. [*Bindschadler et al.*, 1992a, Figure 16].

Tellus records a rich structural history. The eastern and southern margins of Tellus are characterized by a regular structural fabric comprised of long margin-parallel folds and orthogonal grabcn (Figurc 1, locations a). In the south, folds converge in a northwest orientation, oblique to the southern margin (Figure 1, location b). The interior of Tellus hosts basin-and-dome terrain [*Hansen and Willis,* 1996], irregular tessera terrain characterized by arcuate ridges and troughs that define short folds, and graben of various orientations (Figure 1, location c). Tellus' basin-and-dome terrain is generally graben dominated. *Senske*'s [1999] preliminary geologic map of the Tellus Tessera Quadrangle (USGS, V-10) delineates four tessera terrain domains (T1 through T4).

The majority of Tellus is radar-bright, indicating high surface roughness at the scale of the radar wavelength (12.6 cm); however, numerous radar-dark ITBs occur throughout Tellus, ranging from a few kilometers to several hundred kilometers wide. Many large ITBs occur in groups among the folds near the plateau margins (Figure 1, locations d and e). Smaller ITBs occur in the interior basin-and-dome terrain of Tellus (Figure 1, location c). The focus of this study is a large ITB covering ~10,300 km^2 of tessera fabric that occurs near Tellus' eastern margin (Figurc 2). Thc ITB displays volcanic flows preferentially oriented approximately north and east between and around similarly oriented radar-bright tessera kipukas. The resulting ITB resembles a waffle; hence we call it "waffle basin". Although waffle basin volcanic flows occupy local topographic lows, the waffle basin sits along a regional topographic high, one of the highest regions in Tellus. The formation of the waffle basin is the topic of this paper.

3. Geologic Relationships at the Waffle Basin

3.1. Geology

We analyzed digital full-resolution (FMIDR, 75 m/pixel) and compressed (C1MIDR, 225 m/pixel; C2MIDR, 675 m/pixel) synthetic aperture radar (SAR) and GTDR 3:1 altimetry (4.64 km/pixel) Magellan data of the waffle basin region using Interactive Data Language (IDL) and Image 1.62 SXM software. IDL and Image greatly enhanced our ability to characterize lineaments and surfaces by allowing us to interactively stretch the data to selectively enhance particular tonal ranges. Effective resolution of Magellan SAR images varies with latitude and is ~110-125 m at Tellus [*Ford and Plaut*, 1993]. The combined use of cycle 1 and 3 (left-look) versus cycle 2 (right-look) SAR data greatly aids in resolving surface features because features that are not resolved in one look direction might be resolved in the other. We used surface roughness and relative topography estimated from tonal variation in SAR data to constrain surface geology following *Ford et al.* [1993a]. *Stofan et al.* [1993] and *Ford et al.* [1993b] provide guidelines for distinguishing tectonic and volcanic features, respectively, in SAR data. The diameter of the altimeter footprint (the effective horizontal resolution) varies with latitude and is approximately 10-20 km at Tellus. We also used synthetic stereo imaging to explore correlations between altimetry and SAR images in an attempt to understand the regional topographic context [*Kirk et al.*, 1992].

Generally north and east trending structures dominate the tessera fabric at the waffle basin and control ITB shape (Figure 2). The waffle basin floor is likely rough, similar in

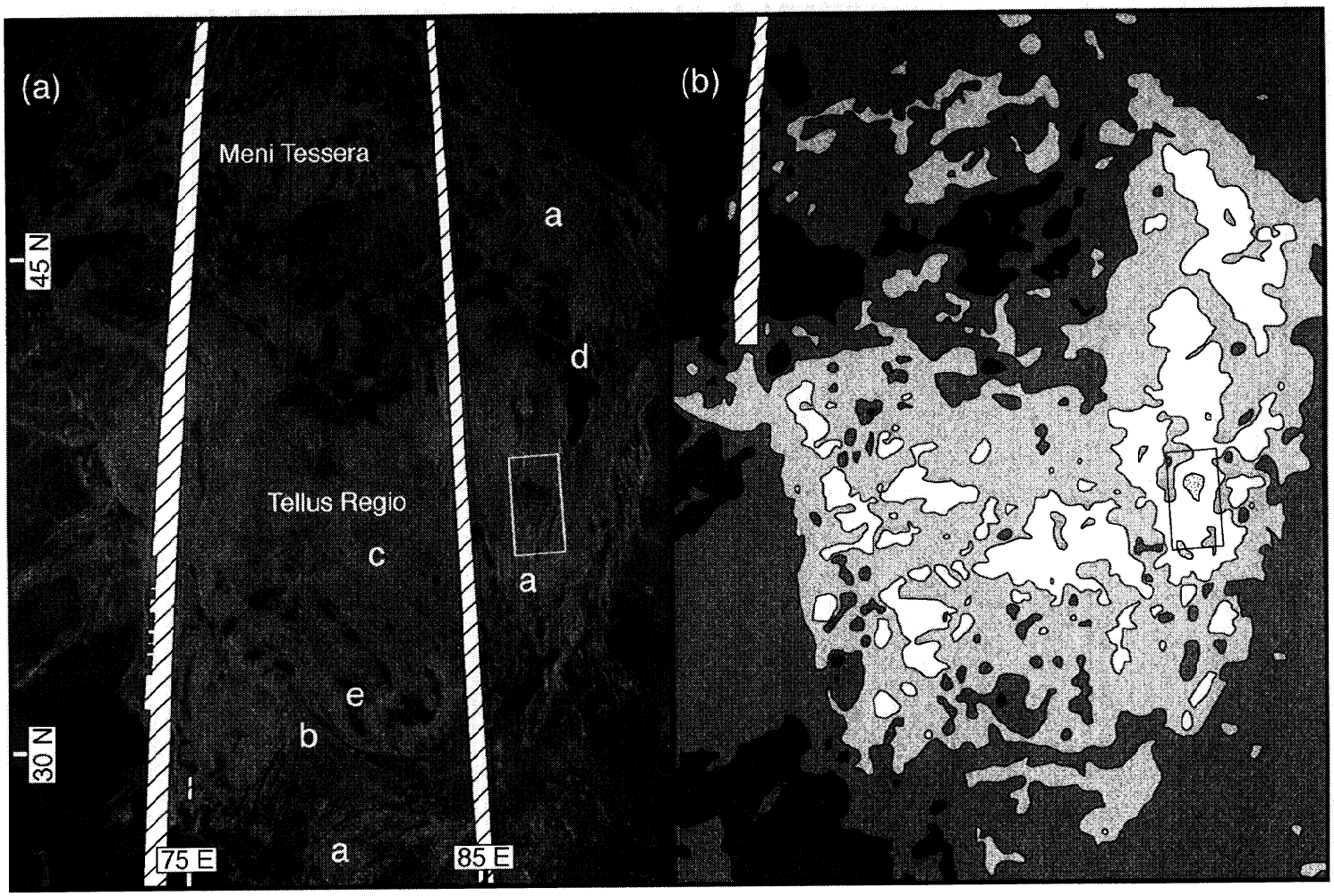

Fig. 1. Banks and Hansen

Figure 1. (a) Tellus synthetic aperture radar (SAR) image forged from Magellan C3-MIDR data. Regional volcanic plains surround radar-bright crustal plateau tessera. Margin-parallel folds occur with orthogonal graben at plateau margins (locations a). Folds converge in a northwest orientation at the southern margin (location b). Short, arcuate graben and folds characterize the Tellus interior (location c). Many radar-dark intratessera flood lava basin (ITB) volcanic deposits occur within tessera (e.g., locations c, d and e). (b) Tellus hypsometry sampled on a 0.5° x 0.5° grid. The rectangles show the location of Figure 2.

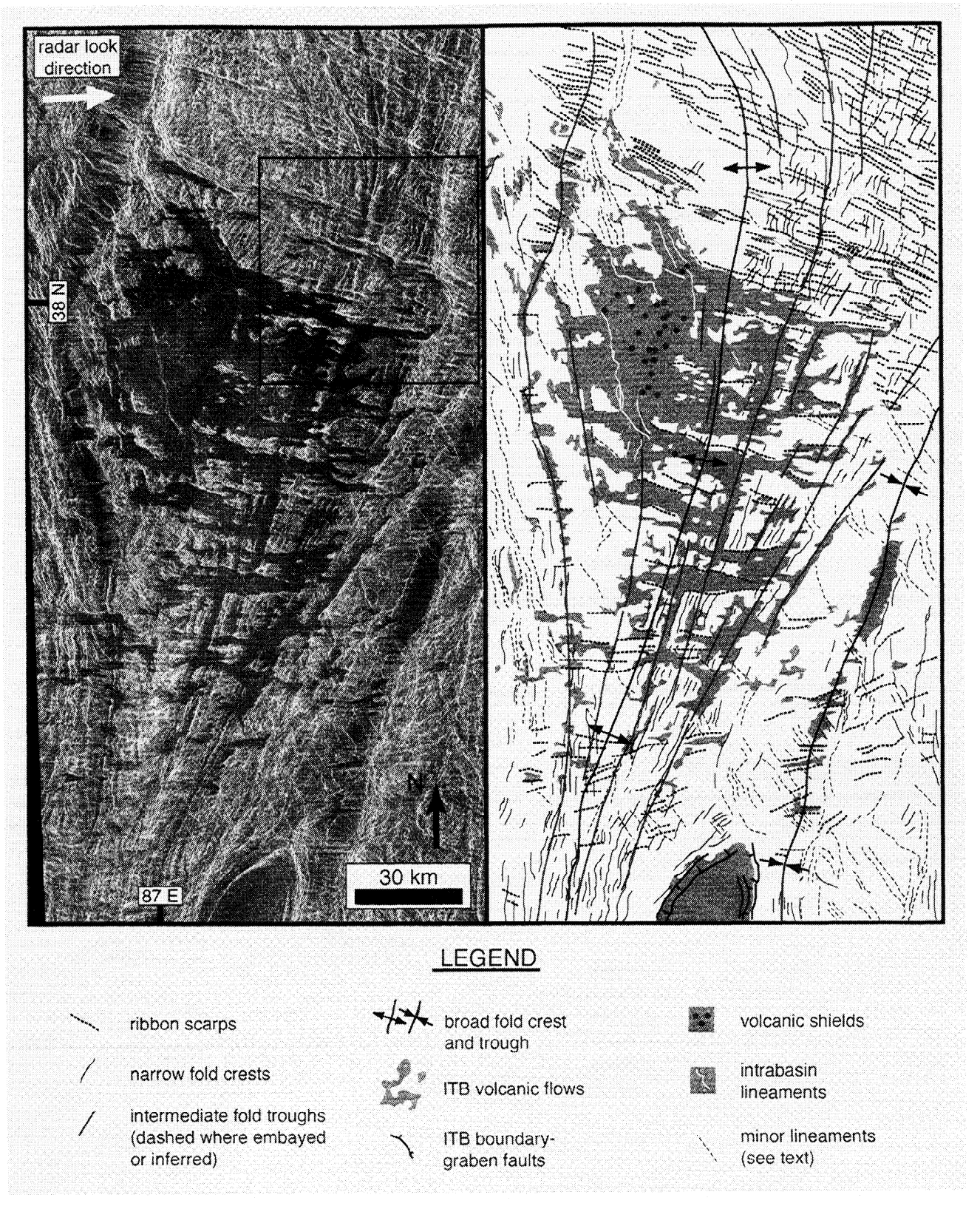

Figure 2. Cycle 1 left-look SAR and generalized geologic map of waffle basin region (enlargement of rectangle in Figure 1). Generally north and east trending radar dark volcanic flows follow dominant trends of secondary structures in the underlying tessera. Major east trending escarpments (red) define structures, including ribbons (λ 1-5 km) and wide ribbons (5-12 km). Major north trending structures include short- (λ<1-5 km) and intermediate- (5-15 km) wavelength folds and a single broad fold. ITB flows embay ribbon and short- to intermediate-wavelength fold troughs. The intermediatc-wavelength fold trough to the west of the basin bends around its widest part. The basin sits perched along the broad fold crest. Box shows the location of Figure 4.

morphology to surrounding tessera, because it represents a preflood surface of exposed tessera contiguous with that now exposed outside of the waffle basin margins and with interior tessera kipukas (Figure 3). The relatively smooth surface of the waffle basin appears significantly less deformed than the surrounding rough tessera fabric. However, the surface of the ITB is not entirely flat. A few generally northwest trending sinuous lineaments and small circular edifices occur locally within the basin (Figure 2). The sinuous lineaments may mark wrinkle ridges, faults, and/or fractures that deform the basin fill. These lineaments possibly result from deformation (reactivation?) along buried tessera structures, or they may represent the uppermost part of tessera structures that were not completely buried by lava flows. We interpret the small circular features as volcanic shields following *Ford et al.* [1993b].

Outside the basin, east trending structures form a penetrative tectonic fabric across the region (Figure 2). These structures are recorded in radar images as sharply defined bright and dark lineaments. They generally trend east but vary in orientation from approximately S60°E in the north, through due east near the center, to N70°E in the south part of the map area. The majority occurs as single bright lineaments spaced from <1 km (resolution limit) to ~5 km apart. Individual lineaments continue uninterrupted for up to 30 km and are traceable through discontinuities for over 100 km along strike without change in orientation. The sharp tonal contrast of the lineaments indicates that they mark abrupt topographic transitions; we interpret them as escarpments.

Morphological interpretation of east trending structures proved difficult because of their general trend subparallel to radar signal trend [*Farr*, 1993]. At the southern end of the basin, they trend approximately parallel to radar and are therefore poorly imaged. North of the basin the lineament radar angle is slightly greater; therefore morphological characterization of the east trending structures is based primarily on those in the north.

Figure 4 shows left- and right-look SAR images of the northeastern portion of the basin where lineament radar angle is maximum. Radar-bright east trending lineaments define radar-facing scarps. Sharp dark lineaments representing scarps facing away from radar are poorly imaged in both look directions, presumably because a lack of radar signal return is lost in the noise, whereas reflection of the radar signal is much stronger. We interpret bright and dark escarpments as oppositely facing normal-fault scarps that result from surface extension orthogonal to fault trends (Figure 4). Minor volcanic flows embay troughs between linears and highlight their trends. Larger volcanic flows obscure tectonic structure morphology in the immediate vicinity of the waffle basin.

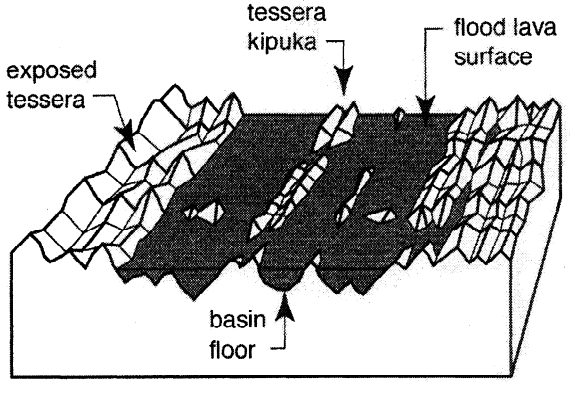

Figure 3. Cartoon block diagram of embayment relationships at the waffle basin. Radar-dark (smooth) ITB volcanic flows embay radar-bright (rough) tessera. Tessera kipukas are preserved locally.

North and south dipping fault scarps form a terrain characterized by long east trending scarp-bounded ridges and troughs. Lineament orientation with respect to radar precludes identification of all trough scarps; thus it is difficult to accurately determine trough spacing. We delineate two suites of trough structures. The dominant suite comprises narrow troughs with a center-to-center trough spacing of 1-5 km. Lineament pairs (one bright and one dark) define narrowly spaced trough walls (Figure 4, profiles a and b). The second suite includes wider troughs with a trough-to-trough spacing of 5 to 12 km. Multiple interior stair-stepped scarps define trough walls of wider troughs (Figure 4, profile c). We interpret the interior scarps as accommodation normal faults. Radar-dark regions, interpreted as volcanic flows, embay some trough floors.

We interpret both suites of troughs as shear-fracture ribbons (narrow, long, straight, steep-sided graben) defined by *Hansen and Willis* [1998]. Shear-fracture ribbons typify crustal plateau tessera terrain and have been described in Thetis [*Hansen and Willis*, 1998], Tellus [*Banks and Hansen*, 1998b], and eastern and western Ovda [*Ghent and Hansen*, 1999] and they also occur in Alpha [K. Bender, personal communication, 1997]. Wide-ribbon troughs of this region are morphologically different from complex graben described elsewhere [e.g., *Hansen and Willis*, 1998; *Ghent and Hansen*, 1999; *Hansen et al.*, 2000]. Wide-ribbon troughs exhibit large length-to-width aspect ratios, whereas complex graben are typically wider and shorter (hence smaller length-to-width aspect ratios). Additionally, wide-ribbon troughs display a regular spacing unlike complex graben [*Pritchard et al.*, 1997; *Ghent and Hansen*, 1999].

North trending structures also form a penetrative tectonic fabric across the region (Figure 2). Generally north trending lineaments vary in orientation from ~N20°W, through north, to N25°E. Individual lineaments are traceable through discontinuities for over 100 km along strike without change in orientation. Lineaments commonly show gradational tonal change across their widths in cycle 1 images, depicting subtle, unidirectional changes in the slope of a curved surface along a line perpendicular to radar look direction (Figure 4, profiles d and e). Bright surfaces sloping toward the radar transition to dark surfaces as they change slope away from the radar. Subtle changes in surface orientation were not clearly imaged in cycle 2, perhaps a result of distortions introduced by small radar incidence angles [*Plaut*, 1993] or the degradation in the quality of cycle 2 images, a result of processing errors [*Ford and Plaut*, 1993].

North trending lineaments define long, narrow alternating ridges and troughs. Ridge-to-ridge spacing varies nearly continuously from <1 km (at radar resolution) to ~15 km. Two ridges of different widths are shown in Figure 4 (profiles d and e). We interpret these ridges and troughs as fold crests and troughs, respectively, owing to the gradational change in radar tone across strike following *Stofan et al.* [1993]. We delineate two suites of ridges: "short-wavelength folds" (ridges spaced from < 1 to 5 km) and "intermediate-wavelength folds" (ridges spaced from 5 to 15 km). Lava flows locally

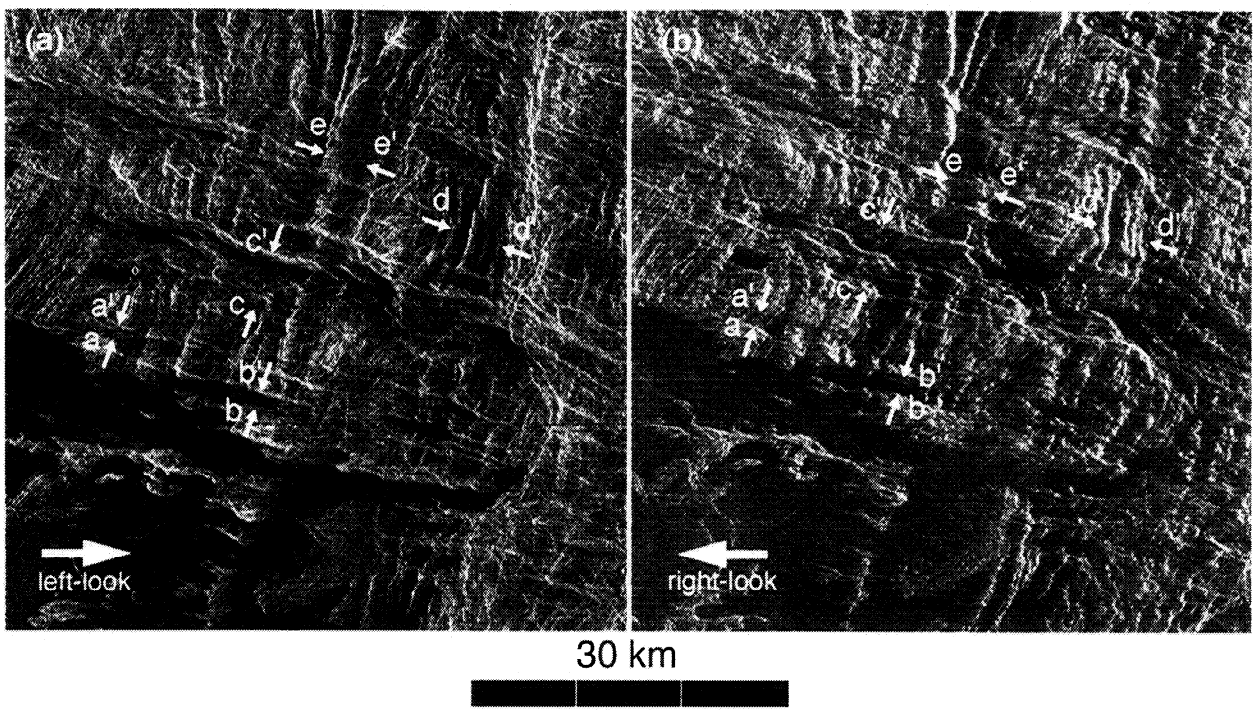

Figure 4. (a) Left-look and (b) right-look SAR images of the northeastern waffle basin margin (enlarged view of box in Figure 2). Generally east trending bright lineaments appear sharp and represent radar-facing normal-fault scarps of shear-fracture ribbons. The majority of the generally north trending lineaments show gradational tonal contrast across their widths and are interpreted as folds. The arrows indicate profile endpoints. (c) Cartoon crosssections showing interpreted topography and geology along selected profiles. Topography is based upon radar tonal changes along profiles. Geology is inferred by structure morphology.

flood some fold troughs (Figure 4, profile d). A partially flooded intermediate-wavelength fold trough along the western basin margin bends around the waffle basin.

Some north trending lineaments show a sharp rather than gradational bright-dark transition. Sharp north-trending lineaments occur predominantly along the western margin of waffle basin. Single sharp lineaments may represent chevron-like folds, thrust-fault scarps, normal-fault scarps, or fractures. They also occur in distinct bright and dark lineament groups that define long stair-stepped troughs. Although we interpret these troughs to be graben, radar resolution does not allow unambiguous interpretation of many sharp north trending lineaments.

A regional view of Tellus' eastern margin reveals another set of north trending topographic features in the vicinity of the waffle basin: broad wavelength ridges and troughs that extend along and parallel to Tellus' eastern margin. These broad-wavelength features trend generally north near the basin, roughly parallel to the short- and intermediate-wavelength folds. The waffle basin lies along the crest of an unusually broad ridge (Figure 1 and Plate 1). Broad north trending troughs lie to the east and west of the basin. The broad ridge width conforms to the width of the basin and the broad trough west of the waffle basin bends around the basin. We interpret the ridge and adjacent troughs as a broad fold consisting of a synform-antiform-synform structure with a

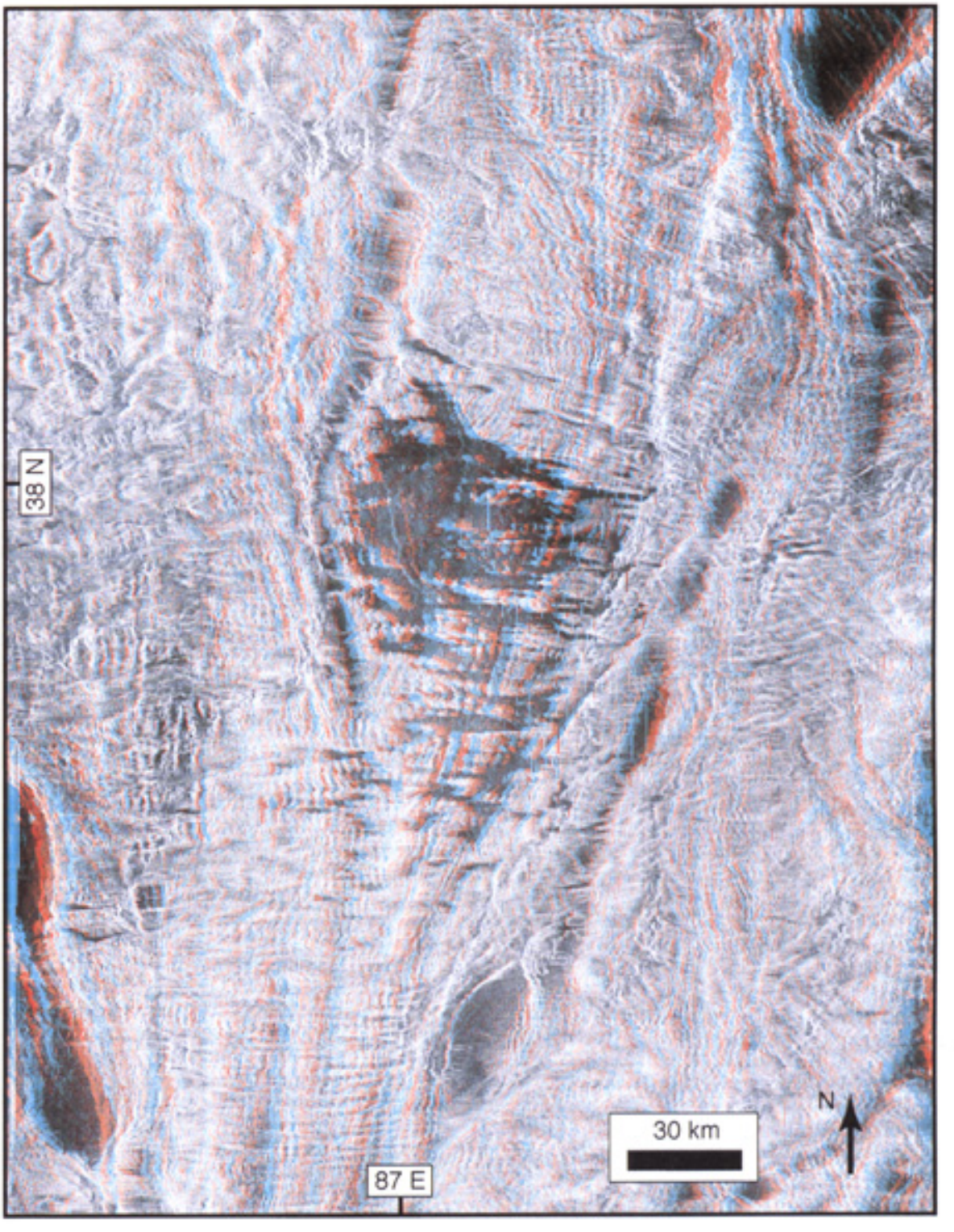

Plate 1. Synthetic stereo image of the waffle basin region prepared following *Kirk et al.* [1992]. View through red- (left eye) and blue-tinted glasses. The waffle basin is situated upon one of two regional topographic ridges (folds) that extend northward.

trough-to-trough spacing of ~65 km at its narrowest and 120 km at its widest, on the basis of altimetry profiles.

In addition to the east and north trending structures described above, we recognize other minor lineaments (Figure 2). Minor lineaments do not dominate the tessera fabric at the waffle basin nor do they form a pervasive pattern across the region. They are, however, locally well developed. Minor lineaments include sharp northwest and north trending lineaments.

Northwest trending lineaments occur predominantly in the southeastern portion of the study area and along the northwestern margin of waffle basin (Figure 2). In both areas the lineaments are sharply defined suggesting that they may represent scarps rather than folds. In the southeast they generally occur as bright-dark lineament pairs that together bound shallow flat-floored troughs. The resulting terrain consists of long alternating ridges and troughs with a trough-to-trough spacing of 4-10 km. We interpret these northwest trending troughs to be shear-fracture ribbons following *Hansen and Willis* [1998]. Northwest trending lineaments at the basin's northwest margin define trough walls with a stair-stepped morphology. These troughs are less abundant, wider, more widely spaced, and deeper than the northwest trending ribbons to the southeast and are composed of multiple interior lineaments. We interpret them to be locally developed graben with multiple interior accommodation faults. These graben are embayed by ITB volcanic flows and control the shape of the basin's northwestern margin.

On the basis of our analysis of Magellan SAR imagery we identified five major tectonic elements within tessera terrain at the waffle basin (Figure 2). East trending lineaments define two sets of shear-fracture ribbons: ribbons (λ 1-5 km) and wide ribbons (λ 5-12 km). North trending structures include short- (λ<1-5 km) and intermediate-wavelength (λ 5-15 km) folds. The waffle basin lies along a broad-wavelength fold crest (λ>100 km) that parallels Tellus' eastern margin. Other minor structural elements that reflect a small portion of the total surface strain in this region also exist.

Senske [1999] mapped a boundary between two types of tessera (T3 and T4) through the northeast corner of the region encompassed in Figure 2. Our map shows a continuity of structural patterns across the region. We find no evidence for a material unit boundary nor do the limits of tectonic structures define such a boundary.

The major tectonic structures identified at the waffle basin resulted from crustal thickening and uplift associated with plateau construction. Ribbons form a unique tectonic fabric common only to crustal plateau tessera terrain [*Hansen and Willis*, 1998; *Ghent and Hansen*, 1999; *Hansen et al.*, 2000], suggesting that they result from processes associated with crustal plateau formation. Cylindrical margin-parallel folds (λ 10-30 km) typify tessera at crustal plateau margins [*Bindschadler and Head*, 1991; *Bindschadler et al.*, 1992b; *Solomon et al.*, 1992; *Ghent and Hansen*, 1999]. In each case the margin-parallel folds are interpreted as the result of margin-normal contraction during crustal plateau genesis. Folds with wavelengths of the order of >100 km, such as the broad fold that hosts the waffle basin, have not previously been identified at other crustal plateau margins. However, because the broad-wavelength fold at the waffle basin parallels shorter-wavelength folds and likewise reflects margin-normal contraction that leads to crustal thickening, we submit that the broad-wavelength fold most likely also represents deformation associated with plateau construction. Additional evidence that these structures result from deformation associated with crustal plateau formation is that their structural patterns correlate with crustal plateau gravity-topography relationships [*Hansen et al.*, 1999].

3.2. Temporal Relationships

Many workers have included the relative timing of ITBs and crustal plateau tectonism in their models, but none have provided geologic analysis to support their proposed timing relationships. *Phillips and Hansen* [1994] suggested that ITBs represent regions of preexisting plains incorporated into crustal plateau tessera as a result of outward migrating deformation belts; this model predicts that ITB magmatism is early with respect to crustal plateau deformation. In contrast, *Ivanov and Head* [1996] proposed that ITB volcanic flows represent plains material which was emplaced over tessera tectonic fabric and thus postdated crustal plateau formation. A third possibility, that ITB volcanism occurred during plateau formation, has not been considered.

Methods for determining relative temporal relationships may be grouped into three major categories: (1) stratigraphic analysis, (2) mechanical analysis, and (3) crosscutting relationships. Stratigraphic analysis uses the principle of superposition to determine relative time between depositional units (i.e., sedimentary or igneous) in the absence of tectonism. Mechanical analysis addresses the timing of secondary structures based on how material units deform and therefore deals with tectonism. Crosscutting relationships provide relative age constraints between material units and secondary structures. (For a more complete discussion, see *Hansen* [2000]). We use crosscutting relationships and mechanical analysis to determine geologic history.

Volcanic flows that erupt to the surface may interact with secondary structures at the surface such that together they can be used to construct a relative temporal framework that is based upon two principles: (1) secondary structures are younger than the material unit(s) they crosscut, and (2) depositional units are younger than the secondary structure(s) they embay. Flows can also completely cover (thus postdate) preexisting secondary structures, such as a fracture suite. In order to use crosscutting relationships to resolve temporal constraints, material units and tectonic structures must be mapped independently.

It may be possible to determine firm temporal relationships between two different material units if tectonism occurs temporally between the emplacement of the units. Without intervening tectonism, such as fracture formation, firm temporal constraints between volcanic units are typically difficult to ascertain. Similarly, the relative timing of two temporally discrete tectonic episodes can be differentiated if volcanism occurs temporally between the tectonic events. Determining temporal relationships between tectonic events is more difficult without intermittent volcanism.

Temporal constraints can also be gleaned from the comparison of material unit patterns with structural patterns. For example, assuming horizontal deposition, if a material unit preferentially occupies synformal fold valleys, it was likely deposited after folding, whereas if the unit map pattern does not correlate with fold patterns, it likely formed prior to folding. Caution is necessary, however, because strain may be recorded differently in adjacent material units owing to

rheological heterogeneity. If a competency contrast is great enough, strain may be partitioned around a strong material unit similar to that of foliation wrapping around a porphyroclast in a dynamically recrystallized metamorphic rock [e.g., *Bell*, 1985]. Such strain partitioning can occur at all scales up to orogenic belts [e.g., *Knipe and Rutter*, 1990; *Seeber and Pecher*, 1998; *Gomez et al.,* 1998]. Rheological differences between a relatively strong porphyroclast and weak matrix cause strain to be partitioned differently within each medium. Therefore, even if the shape of a material unit correlates with structural patterns at its boundaries, the material unit may have existed prior to tectonism. In such cases, structure morphology (e.g., size, shape, spacing, and trend) should provide clues as to the influence of strain partitioning.

Possible structural reactivation, renewed slip along previously formed mechanical discontinuities, must also be considered. Once formed, a structure has the potential to be a material weakness. Whether a preexisting structure is reactivated depends on the character of the structure,and, in large part, on its orientation with respect to future (younger) operative principal stresses [*Sibson*, 1985; *Twiss and Moores*, 1992, pp. 169-185].

Crosscutting relationships between crustal plateau tectonic structures and ITB volcanic flows can provide clues to surface evolution. If ITB magmatism entirely predated plateau tectonism, ITB flows should not embay crustal plateau structures, and crustal plateau structures might cut the flows. If plateau formation predated ITB volcanism, ITB flows should embay local tessera lows and not exist at high topographic levels. If ITB volcanism occurred during plateau formation, ITB flows should embay preexisting plateau structures, and be cross cut or affected by late structures.

At the waffle basin, volcanic flows locally embay the troughs of ribbons and short-wavelength folds; however, there is no evidence that either ribbons or short-wavelength folds cross -cut waffle basin flows. Therefore,- it is reasonable to interpret that most of the basin volcanism occurred after the formation of these short wavelength structures.

In contrast, an intermediate-wavelength fold trough bends around the western margin of the waffle basin (Figure 2), suggesting that the waffle basin influenced shortening patterns, a consequence of strain partitioning or barreling. The waffle basin was apparently more competent than its surroundings and therefore influenced the location of the intermediate wavelength folds in the area. The increase in strength at the location of the waffle basin could result from a combination of the lateral extent of basin fill and the local increase in thickness as a result of basin fill. The basin appears to have been filled by low-viscosity lava and, as such, likely represented a relatively flat surface at the time of lava emplacement. Lava cooling and solidification lead to a local strengthening of the basin region. The strengthening envisioned would be similar to the local strengthening of a piece of cross-corduroy fabric on which glue was allowed to fill the spaces between the corduroy ridges. A local strengthening could also be related, in part, to a cooled and solidified magmatic intrusion at depth related to the surface volcanic pile. Whatever the cause, the regional rheological heterogeneity at the waffle basin has temporal implications. In order for the basin to have influenced intermediate-wavelength fold trends the magmatic basin must have existed, at least in part, prior to intermediate-wavelength fold formation. Intermediate-wavelength folds are also partially buried by volcanic flows, indicating that volcanism continued after intermediate-wavelength fold formation.

The broad-wavelength fold troughs also bend around the widest part of the waffle basin (Plate 1), indicating that the strain associated with broad-fold formation was partitioned by the existence of the waffle basin and therefore formed during or after basin formation. If volcanism occurred after broad-fold formation, low-viscosity flood lava should have flowed down local ribbon troughs to broad-fold troughs. Although the synformal troughs are not filled with lava, current image resolution does not allow one to determine whether or not some lava flowed down the limb of the fold. The lack of spatial correlation of lava flooding within broad synformal troughs is also consistent with early ITB volcanism and late broad fold formation. Therefore geologic relations are most consistent with the interpretation that the waffle basin was uplifted on the broad-fold crest after the basin formed. This temporal interpretation is also consistent with the nonplaner orientation of the surface of the waffle basin fill as seen in synthetic stereo.

Crosscutting relationships indicate the following geologic sequence at the waffle basin: (1) ribbon and short-wavelength fold formation, (2) lava flooding, (3) intermediate-wavelength fold formation, (4) continued lava flooding, and (5) uplift of basin along the broad wavelength fold. Mechanical arguments further constrain waffle basin geologic history and allow us to track the competent layer thickness at the waffle basin through time.

Using consistency arguments, it may be possible to constrain relative temporal relationships between mutually crosscutting tectonic structures through an understanding of their kinematic relationships. Strain theory provides the foundation for interpreting homogeneous strain patterns using the finite strain ellipse whose principal axes record maximum and minimum longitudinal strain [*Ramsay and Huber*, 1983, 1987; *Price and Cosgrove*, 1990]. In an environment represented by a single strain ellipse, contractional, extensional, and strike-slip structures can form synchronously with geometric relationships between structures determined by the principal strain axes. If structures have kinematic relationships consistent with a single strain ellipse, they may have formed synchronously. For example, *Ramberg* [1959] showed that folds (contractional) and boudins (extensional) can develop simultaneously in response to the same bulk stress regime. At the waffle basin the orthogonal relationship of east trending ribbons (extensional) and north trending folds (contractional) is consistent with a single bulk strain regime, consistent with synchronous formation.

Mechanical arguments can also constrain competent layer thickness based on structural wavelength; the thickness of a competent layer affects the wavelength of the resulting structures—the thicker the competent layer, the longer the structural wavelength [*Ramberg*, 1959; *Huddleston and Lan*, 1995]. We calculated the maximum layer thickness associated with the folds at the waffle basin following *Ghent and Hansen* [1999, and references therein] using an empirical fold wavelength-to-layer thickness ratio of 3:1. Similarly, we determined the layer thickness associated with ribbons following *Hansen and Willis* [1998, and references therein] using a ribbon wavelength-to-layer thickness ratio of 3:1. Similar wavelengths of ribbons and short-wavelength folds indicate that they likely deformed a similarly thin (<2 km)

Table 1. Compilation of Structural Data for Waffle Basin Structures

Structure	Trend	Wavelength, km	Strain Type	Layer Thickness, km
Ribbons	east	1-5	extension	<2
Wide ribbons	east	5-12	extension	<4
Short folds	north	<1-5	shortening	<2
Intermediate folds	north	5-15	shortening	<5
Broad fold	north	65-120	shortening	>5

competent layer (Table 1). Experimental studies show that synchronous formation of orthogonal extensional faults and contractional folds of a competent single layer yields slightly longer wavelength extensional structures [*Kobberger and Zulauf*, 1995]. Likewise, wide ribbons and intermediate wavelength folds have a similar spacing and likely deformed a somewhat thicker (<5 km) competent layer. One interpretation consistent with the data is that east trending ribbons and short-wavelength folds first deformed a thin (<2 km) competent layer. Later, as the competent layer thickened (<5 km) with time, continued deformation in an identical bulk strain regime formed more widely spaced (longer wavelength) ribbons and folds. If the crust was layered, it is also possible that the two suites of ribbons and the short- and intermediate-wavelength folds formed generally synchronously, whereby the narrowly spaced structures deformed only the upper layer(s) while the more widely spaced structures deformed a thicker competent package. The broad-wavelength fold deformed a much thicker competent layer than did the narrower-wavelength structures (Table 1).

3.3. Geologic History

Early tectonism at the waffle basin involved orthogonal extension (north directed) and contraction (east directed) of a thin competent layer, developing a pervasive fabric consisting of ribbons and short wavelength folds (Figure 5,

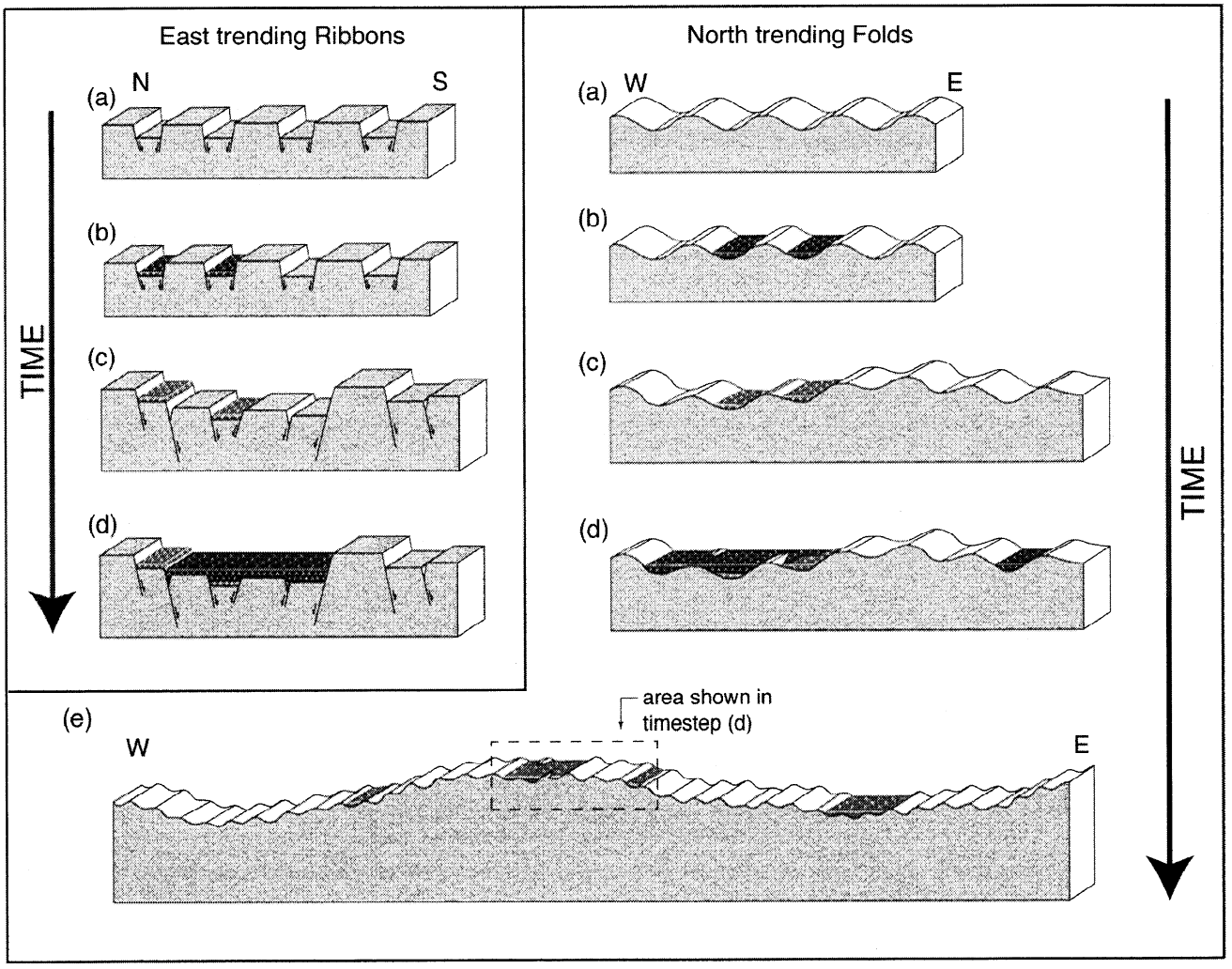

Figure 5. Cartoon block diagrams depicting surface evolution at the waffle basin. East trending ribbons and north trending folds (time step a) deform a thin competent layer. Limited local lava floods some ribbon and short-wavelength fold troughs (carrot pattern) (time step b). Continued orthogonal extension and contraction of a thicker competent layer results in formation of wide ribbons and intermediate-wavelength folds (time step c). Major episode of ITB volcanism embays early formed ribbon and fold troughs (time step d). Preexisting lava flows (medium gray) may or may not be covered by new flows. Contraction of a locally thickened and laterally strengthened thick competent layer uplifts the waffle basin (tie step e).

time step a). Flood lava locally filled ribbon and short-wavelength fold troughs (Figure 5, time step b). As the depth to the brittle-ductile transition increased, continued orthogonal extension and contraction led to the development of more widely spaced wide ribbons and intermediate-wavelength folds (Figure 5, time step c). By that time, volcanic flows had imparted a rheological heterogeneity to the region that influenced intermediate-wavelength fold trends such that they bend around the basin. Volcanism continued subsequent to wide ribbon and intermediate wavelength fold formation as evidenced by the lack of ribbons and folds that cut basin flows (Figure 5, time step d). Continued (possibly) margin-normal contraction accompanied by an increase in competent layer thickness formed a broad-wavelength fold that uplifted the waffle basin into a position along the crest of a regional antiform (Figure 5, time step e).

Determining the relationship between strain and stress is a complicated matter, especially in an anisotropic and heterogeneous medium such as the Venusian lithosphere. Even if Venus' lithosphere were compositionally uniform, mechanical elements (folds, faults, and fractures) that developed in response to early stresses could control or affect subsequent expressions of strain (folds, faults, and fractures). For example, *Ghosh* [1988] applied a thin layer of plaster of Paris to the top of a slab of pitch and allowed it to extend under the influence of gravity. He introduced a lineation to the surface by brushing the plaster of Paris onto the pitch and found that the orientation of the anisotropy, rather than the principal stress directions, determined the orientation of subsequently formed fractures. Similarly, at waffle basin, early formed ribbons and folds may have imparted a mechanical heterogeneity to the crust that influenced the orientation of later formed structures. Because of this, principal stress directions could have rotated considerably while principal finite strain axes remained unchanged. Ribbon and fold structure orientations indicate that the maximum and minimum directions of extension at the waffle basin were oriented north (parallel to plateau margin) and east, respectively, throughout much of Tellus' formation (Figure 6). Although minor structures at waffle basin may be inconsistent with this bulk strain, they could represent local perturbations in the regional strain pattern. Despite the apparent uniform strain regime, the direction of maximum compression (i.e., stress) could have varied considerably through plateau evolution (Figure 6).

The geologic history that emerges reflects the evolution of a surface with generally synchronous north directed extension and east directed contraction that persisted through time punctuated by multiple episodes of local flood lava volcanism. Local topography resulting from extension and contraction of the surface was ever changing. Local lava flows that filled existing local lows were deformed by subsequent tectonism. The overall strength of the crust was presumably a result of increased thickness with time, such that longer-wavelength structures postdate shorter-wavelength structures. Fold wavelength increased with time, yet the fold axes retained a general north trend. Similarly, it is likely that ribbon troughs, which also retained generally parallel trends, became more widely spaced with time.

4. Implications for Crustal Plateau Models

Temporal relationships at the waffle basin indicate that volcanism occurred during crustal plateau formation. ITB volcanic flows embay ribbons and folds that comprise early tessera fabric, and therefore they cannot represent preexisting plains captured by crustal plateau deformation as suggested by *Phillips and Hansen* [1994]. Intermediate- and broad-wavelength folds bend around the waffle basin, such that the basin must have existed, at least in part, prior to the formation of these folds. Moreover, a broad plateau margin fold apparently uplifted the ITB onto its crest. Therefore ITB magmatism could not have completely or dominantly postdated crustal plateau construction as proposed by *Ivanov and Head* [1996]. Instead, waffle basin volcanism must have accompanied crustal plateau formation. If the timing of the waffle basin with respect to crustal plateau construction typifies ITBs as we suspect, then magmatism likely played a major role in crustal plateau formation. More detailed geological studies aimed at resolving temporal relationships at other ITBs are needed to test this hypothesis.

Workers proposed mantle downwelling for crustal plateau formation to explain folds within tessera terrain initially resolved in Venera images and confirmed in Magellan SAR imagery [*Bindschadler and Parmentier*, 1990; *Bindschadler et*

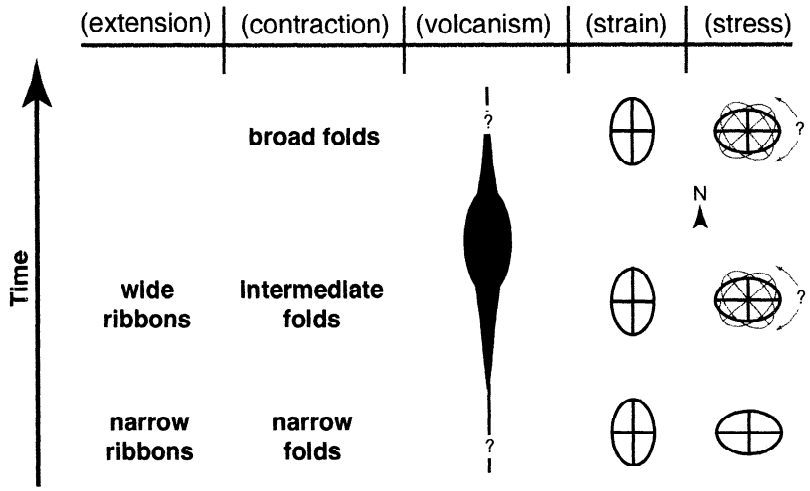

Figure 6. Time line of the surface evolution at waffle basin.

al., 1992a]. In the downwelling model, subsolidus flow of lower crustal material, initiated by the negative buoyancy of a mantle coldspot, results in crustal thickening. As downwelling wanes, negative dynamic support is lost, and gravitational slumping of overly thickened crust results in extensional deformation that overprints folds. This model, which predicts early surface contractional strain, does not explain the occurrence of widespread ribbon formation (extension) that predates long-wavelength folds [*Hansen and Willis*, 1996, 1998; *Ghent and Hansen*, 1999]. A revised upwelling model [*Hansen and Willis*, 1998; *Phillips and Hansen*, 1998] calls upon a deep mantle plume to heat and anneal the initially thin lithosphere above the plume head. Magmatic accretion results in early widespread surface extension of a thin surface "scum" of the thermally annealed lithosphere, forming ribbons. Magmatic underplating thickens the crust, and margin-parallel folds form as crustal material gathers at plateau margins. As the thermal plume subsequently decays, deflation of the interior region causes interference folding and/or local extensional collapse. Late stage extension may result from gravitational collapse of uplifted crust as thermal support is lost. The revised upwelling model for crustal plateau formation better explains the entire suite of observed structures, their temporal relationships, and the steep-sided, flat-topped morphology characteristic of crustal plateaus [*Hansen et al.*, 1999, 2000].

The geologic history discerned at the waffle basin is consistent with the upwelling model in which early surface extension and early volcanism would be expected in a hotspot environment. Conversely, early widespread extension and volcanism would not be expected by the downwelling model because (1) horizontal, radial convergence predicted by this model would presumably obstruct early surface extension and (2) the lower than normal geothermal gradients would impede, rather than enhance, volcanism.

5. Conclusions

In order to evaluate the significance of ITB volcanic deposits with respect to crustal plateau evolution we asked the question, Did waffle basin magmatism occur before, during, or after local crustal plateau tectonism? Geologic relationships at the waffle basin indicate that ITB volcanism occurred during crustal plateau formation. Although additional geological studies are required to determine the relative timing of other ITBs, we extend the timing relationships resolved at the waffle basin to other Tellus ITBs. We suggest that abundant ITB magmatism occurred during crustal plateau construction and thus played a major role in crustal plateau genesis. Widespread volcanism is expected in an upwelling environment. Therefore this work provides further evidence that supports the new upwelling model of crustal plateau formation. This study further supports the hypothesis that Venus' crustal plateaus may be analogous in many regards to terrestrial oceanic plateaus [*Hansen et al.*, 1999].

Acknowledgments. NASA's Planetary Geology and Geophysics program supported this work under grants NAGW-2915 and NAG5-4562 to Southern Methodist University. We thank L. Bleamaster, H. DeShon, G. Eisenstadt, B. Ghent, J. Goodge, D. Oliver, B. Stump, and D. Young for fruitful discussions. We thank R. Buck, S.Smrekar, and an anonymous reviewer for their comments.

References

Banerdt, W. B., M. E. McGill and M. T. Zuber, Plains tectonics on Venus, in *Venus II*, edited by S. W. Bougher, D. M. Hunten, and R. J. Phillips, pp. 901-930, University of Arizona Press, Tucson, 1997.

Banks, B. K., and V. L. Hansen, Intra-tessera flood-lava basins on Venus (abstract), *Geol. Soc. Am. Abstr. Programs*, *30*, 7, 1998a.

Banks, B. K., and V. L. Hansen, Chocolate tablet boudinage on Venus (abstract), *Proc. Lunar Planet. Sci. Conf.*, *29*, 1449-1450, 1998b.

Banks, B. K., and V. L. Hansen, Intratessera flood-lava basins (ITBs) constrain timing of crustal plateau structures (abstract), *Proc. Lunar Planet. Sci. Conf.*, *30*, 1253-1254, 1999.

Barsukov, V. L., et al., The geology and geomorphology of the Venus surface as revealed by the radar images obtained by Veneras 15 and 16, *Proc. Lunar Planet. Sci. Conf.* 16th, Part 2, *J. Geophys. Res.*, *91*, suppl., D378-D398, 1986.

Basilevsky, A. T., A. A. Pronin, L. B. Ronca, V. P. Kryuchkov, A. L. Sukhanov, and M. S. Markov, Styles of tectonic deformations on Venus: Analysis of Venera 15 and 16 data, *Proc. Lunar Planet. Sci. Conf.* 16th, part 2, *J. Geophys. Res.*, *91*, suppl., D399-D411, 1986.

Bell, T. H., Deformation partitioning and porphyroblast rotation in metamorphic rocks: A radical reinterpretation, *J. Metamorph. Geol.*, *3*, 109-118, 1985.

Bindschadler, D. L., and J. W. Head, Diffuse scattering on the surface of Venus: Origin and implications for the distribution of soils, *Earth Moon Planets*, *42*, 133-149, 1988.

Bindschadler, D. L., and J. W. Head, Tessera terrain, Venus: Characterization and models for origin and evolution, *J. Geophys. Res.*, *96*, 5889-5907, 1991.

Bindschadler, D. L., and E. M. Parmentier, Mantle flow tectonics: The influence of a ductile lower crust and implications for the formation of topographic uplands on Venus, *J. Geophys. Res.*, *95*, 21,329-21,344, 1990.

Bindschadler, D. L., G. Schubert, and W. M. Kaula, Coldspots and hotspots: Global tectonics and mantle dynamics of Venus, *J. Geophys. Res.*, *97*, 13,495-13,532, 1992a.

Bindschadler, D. L., A. deCharon, K. K. Beratan, S. E. Smrekar, and J. W. Head, Magellan observations of Alpha Regio: Implications for formation of complex ridged terrains on Venus, *J. Geophys. Res.*, *97*, 13,563-13,578, 1992b.

Farr, T. G., Radar interactions with geologic surfaces, in *Guide to Magellan Image Interpretation*, edited by J. P. Ford et al., *JPL Publ.*, *93*(24), 45-56, 1993.

Ford, J. P., and J. J. Plaut, Magellan image data, in *Guide to Magellan Image Interpretation*, edited by J. P. Ford et al., *JPL Publ.*, *93*(24), 7-18, 1993.

Ford, J. P., J. J. Plaut, C. M. Weitz, T. G. Farr, D. A. Senske, E. R. Stofan, G. Michaels, and T. J. Parker, (Eds.), *Guide to Magellan Image Interpretation, JPL Publ. 93*(24), Jet Propul. Lab., Pasadena, Calif., 1993a.

Ford, J. P., J. J. Plaut, and T. J. Parker, Volcanic features, in *Guide to Magellan Image Interpretation*, edited by J. P. Ford et al., *JPL Publ.*, *93*(24), 109-134, 1993b.

Ghent, R. R., and V. L. Hansen, Structural and kinematic analysis of eastern Ovda Regio, Venus: Implications for crustal plateau formation, *Icarus*, *139*, 116-136, 1999.

Ghosh, S. K., Theory of chocolate tablet boudinage, *J. Struct. Geol.*, *10*, 541-553, 1988.

Gilmore, M. S., and J. W. Head, The formation and evolution of Alpha and Tellus tesserae on Venus (abstract), *Lunar Planet. Sci.*, XXIV, 533-534, 1993.

Gilmore, M. S., and J. W. Head, Intratessera volcanism of Alpha and Tellus tesserae on Venus (abstract), *Lunar Planet. Sci.*, XXV, 425-426, 1994.

Gomez, F., R. Allmendinger, and M. Dahmani, Crustal shortening and vertical strain partitioning in the Middle Atlas Mountains of Morocco, *Tectonics*, *17*, 520, 1998.

Grimm, R. E., The deep structure of Venusian plateau highlands, *Icarus*, *112*, 89-103, 1994.

Hansen, V. L., Geologic mapping tectonic planets, *Earth Planet. Sci. Lett.*, *176*, 527-542, 2000.

Hansen, V. L., and J. J. Willis, Structural analysis of a sampling of tesserae: Implications for Venus geodynamics, *Icarus*, *123*, 296-312, 1996.

Hansen, V. L., and J. J. Willis, Ribbon terrain formation, southwestern

Fortuna Tessera, Venus: Implications for lithosphere evolution, *Icarus*, *132*, 321-343, 1998.

Hansen, V. L., J. J. Willis, and W. B. Banerdt, Tectonic overview and synthesis, in *Venus II*, edited by S. W. Bougher, D. M. Hunten, and R. J. Phillips, pp. 797-844, University of Arizona Press, Tucson, 1997.

Hansen, V. L., B. K. Banks, and R. R. Ghent, Tessera terrain and crustal plateaus, Venus, *Geology*, *27*, 1071-1074, 1999.

Hansen, V. L., R. J. Phillips, J. W. Willis, and R. R. Ghent, Structures in tessera terrain: Issues and answers, *J. Geophys. Res.*, *105*, 4135-4152, 2000.

Head, J. W., Processes of crustal and depleted mantle layer loss on Venus: Evidence from basins in tesserae, uplands, and plains, *Lunar Planet. Sci., XXVI*, 577-578, 1995.

Head, J. W., L. S. Crumpler, and J. C. Aubele, Venus volcanism: Classification of volcanic features and structures, associations, and global distribution from Magellan data, *J. Geophys. Res.*, *97*, 13,153-13,197, 1992.

Huddleston, P. J., and L. Lan, Rheological information from geological structures, *Pure Appl. Geophys.*, *145*, 607-620, 1995.

Ivanov, M. A., and J. W. Head, Tessera terrain on Venus: A survey of the global distribution, characteristics, and relation to surrounding units from Magellan data, *J. Geophys. Res.*, *101*, 14,861-14,908, 1996.

Kaula, W. M., Venus: A contrast in evolution to Earth, *Science*, *247*, 1191-1196, 1990.

Kidan, T. W., and J. W. Cosgrove, The deformation of multilayers by layer-normal compression: An experimental investigation, *J. Struct. Geol.*, *18*, 461-474, 1996.

Kirk, R. L., L. A. Soderblom, and E. M. Lee, Enhanced visualization for interpretation of Magellan radar data: Supplement to the Magellan special issue, *J. Geophys. Res.*, 97, 16371-16380, 1992.

Knipe, R. J. and E. H. Rutter, (Eds.), *Deformation Mechanisms, Rheology and Tectonics, Geol. Soc. Spec. Publ.*, 54, 535 pp., London, 1990.

Knipe, R. J. and E. H. Rutter, (Eds.), *Deformation Mechanisms, Rheology and Tectonics, Geol. Soc. Spec. Publ., 54*, 535pp., London, 1990.

Kobberger, G., and G. Zulauf, Experimental folding and boudinage under pure constrictional conditions, *J. Struct. Geol.*, *17*, 1055-1063, 1995.

Phillips, R. J., and V. L. Hansen, Tectonic and magmatic evolution of Venus, *Annu. Rev. Earth Planet. Sci.*, *22*, 597-654, 1994.

Phillips, R. J., and V. L. Hansen, Geological evolution of Venus: Rises, plains, plumes, and plateaus, *Science*, *279*, 1492-1497, 1998.

Plaut, J. J., Stereo imaging, in *Guide to Magellan Image Interpretation*, edited by J. P. Ford et al., *JPL Publ.*, *93*(24), 33-43, 1993.

Price, N. J., and J. W. Cosgrove, *Analysis of Geological Structures*, Cambridge Univ. Press, New York, 1990.

Pritchard, M. E., V. L. Hansen, and J. J. Willis, Structural evolution of western Fortuna Tessera, Venus, *Geophys. Res. Lett.*, *24*, 2339-2342, 1997.

Ramberg, H., Evolution of ptygmatic folding, *Nor. Geol. Tidsskr.*, *39*, 99-152, 1959.

Ramsay, J. G., and M. I. Huber, *The Techniques of Modern Structural Geology, vol. 1, Strain Analysis*, Academic, San Diego, Calif., 1983.

Ramsay, J. G., and M. I. Huber, *The Techniques of Modern Structural Geology, vol. 2: Folds and Fractures*, Academic, San Diego, Calif., 1987.

Seeber, L., and A. Pecher, Strain partitioning along the Himalayan arc and the Nanga Parbat antiform, *Geology*, *26*, 791-794, 1998.

Senske, D. A., Geology of the Tellus Tessera quadrangle (V-10), Venus (abstract), *Proc. Lunar Planet. Sci. Conf.*, *30*, 1668, 1999.

Sharpton, V. L., and J. W. Head, Analysis of regional slope characteristics on Venus and Earth, *J. Geophys. Res.*, *90*, 3733-3740, 1985.

Sibson, R. H., A note on fault reactivation, *J. Struct. Geol.*, *7*, 751-754, 1985.

Simons, M., S. C. Solomon, and B. H. Hager, Localization of gravity and topography: Constraints on the tectonics and mantle dynamics of Venus, *Geophys. J. Int.*, *131*, 24-44, 1997.

Smrekar, S. E., and R. J. Phillips, Venusian highlands: Geoid to topography ratios and their implications, *Earth Planet. Sci. Lett.*, *107*, 582-597, 1991.

Solomon, S. C., J. W. Head, W. M. Kaula, D. McKenzie, B. Parsons, R. J. Philips, G. Schubert, and M. Talwani, Venus tectonics: Initial analysis from Magellan, *Science*, *46*, 48-55, 1992.

Stofan, E. R., D. A. Senske, and G. Michaels, Tectonic features in Magellan data, in *Guide to Magellan Image Interpretation*, edited by J. P. Ford et al., *JPL Publ.*, *93*(24), 93-108, 1993.

Twiss, R. J., and E. M. Moores, *Structural Geology*, W. H. Freeman, New York, 1992.

B. K. Banks, Law Engineering and Environmental Services, Inc., 3301 Atlantic Avenue, Raleigh, NC 27619. (bkbanks@hotmail.com)

V. L. Hansen, Department of Geological Sciences, Southern Methodist University, 3225 Daniel Avenue, Dallas, TX 75275-0395. (vhansen@mail.smu.edu)

(Received October 21, 1999; revised May 15, 2000;
accepted May 17, 2000.)